Stability at High Performance in the MAST Spherical Tokamak

R. J. Buttery, R. Akers, E. Arends 1), N. J. Conway, G. F. Counsell, G. Cunningham, C. G. Gimblett, M. Gryaznevich, R. J. Hastie, M. J. Hole, I. Lehane, R. Martin, A. Patel, T. Pinfold, O. Sauter 2), D. Taylor, G. Turri, M. Valovic, M. J. Walsh 3), H. R. Wilson and the MAST team.

EURATOM/UKAEA Fusion Association, Culham Science Centre, OX14 3DB. UK.
1) FOM Instituut voor plasmafysica "Rijnhuizen", 3430 BE Nieuwegein, The Netherlands.
2) CRPP, Association EURATOM-Confédération Suisse, EPFL, 1015 Lausanne, Switzerland.
3) Walsh Scientific Ltd., Culham Science Centre, Abingdon, Oxon, OX143EB, UK

Email contact of main author: richard.buttery@ukaea.org.uk

Abstract. The development of reliable H-modes on MAST, together with advances in heating power and a range of powerful diagnostics, has provided a platform to enable MAST to address some of the most important issues of tokamak stability. In particular the high β potential of the ST is highlighted with stable operation at β_N ~5-6, β_T~16% and β_p as high as 1.9, confirmed by a range of profile diagnostics. Calculations indicate that β_N levels are in the vicinity of no-wall stability limits. Studies have provided the first identification of the Neoclassical Tearing Mode (NTM) in the ST, using its behaviour to quantitatively validate predictions of NTM theory, previously only applied to conventional tokamaks. Experiments have demonstrated that sawteeth play a strong role in triggering NTMs - by avoiding large sawteeth much higher β_N can, and has, been reached. Further studies have confirmed the NTM's significance, with large islands observed using the 300 point Thomson diagnostic, and locking of large n=1 modes frequently leading to disruptions. H-mode plasmas are also limited by ELMs, with confinement degraded as ELM frequency rises. However, unlike the conventional tokamak, the ELMs in high performing regimes on MAST ($H_{IPB98Y2}$~1) appear to be type III in nature. Modelling identifies instability to peeling modes, consistent with a type III interpretation, and shows considerable scope to raise pressure gradients (despite n=∞ ballooning theory predictions of instability) before ballooning type modes (perhaps associated with type I ELMs) occur. Finally sawteeth are shown not to remove the q=1 surface in the ST - other promising models are being explored. Thus research on MAST is not only demonstrating stable operation at high performance levels, and developing methods to control instabilities; it is also providing detailed tests of the stability physics and models applicable to conventional tokamaks, such as ITER.

1. Introduction

The new generation of Spherical Tokamaks (STs) provides the first opportunity to examine their stability properties in power plant relevant scenarios. This is important in assessing the ST's potential. It also provides critical tests of conventional tokamak physics, as we find that many of the instabilities of the ST are similar to those in the conventional tokamak. The MAST device (major radius 0.85m, minor radius 0.65m, and presently up to 1.5MA plasma current and 3MW neutral beam additional heating) was the first of the new generation of STs to come on line, and its status is described in Ref [1]. Stability studies have benefited from a range of powerful diagnostics, including 300 spatial point (and 20 point multi-time) Thomson scattering, multi-chord Z-effective from visible bremsstrahlung, charge exchange, soft X-ray (SXR), and extensive magnetic arrays, including a new locked mode detector.

Thus MAST has provided the first identification of Neoclassical Tearing Modes (NTMs) in the ST and explorations of their physics and effects. By removal of sawteeth it has been possible to avoid NTMs and achieve much higher β values, where performance has been compared with calculated ideal MHD stability limits. The role of tearing modes in leading to disruptions has also been explored, and the role of error fields identified. Sawtooth behaviour and consequences have been studied. Finally the stability of the edge pedestal has been calculated and used to interpret ELM phenomena. In all of these areas, behaviour is being compared against conventional tokamak physics models to help identify the physics mechanisms on both variants of the tokamak.

2. Neoclassical tearing modes

A key attribute predicted for the ST is access to high plasma pressures at relatively low toroidal field (high β), based on arguments relating to ideal magnetohydrodynamic (MHD) stability. It was borne out by the collisional START device, where β values up to 40% were obtained [2]. However, conventional tokamaks are often limited by NTMs, which occur below the ideal MHD β limit in hot, low collisionality plasmas. By careful choice of plasma regime it has been possible to trigger NTMs on MAST, providing the first identification and explorations of their physics in the ST [3].

As in conventional tokamaks, NTMs in the ST are most easily excited by sawteeth. A typical example is shown in Fig 1, where successive sawteeth (appearing on SXR signals) excite first a 3/2 then a 2/1 NTM

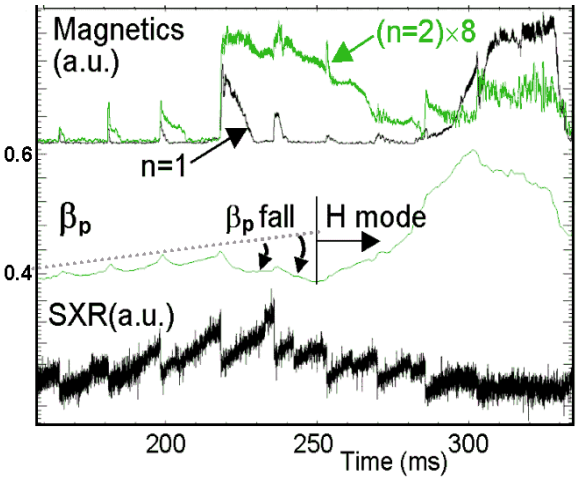

Fig 2: Critical β_p required to excite NTMs

More detailed analysis has shown that behaviour is well described by the usual NTM theory [4]. This is highlighted in Fig 3, where we see the β_p dependence of the 3/2 NTM reflects its bootstrap drive. The complete stabilisation at 280ms shows the role of small island stabilisation terms. This can be provided either by finite transport effects reducing the bootstrap hole in small islands (w_d model), or by an assumed stabilising effect from ion polarisation currents, due to island rotation in the ExB=0 frame of reference (w_{pol} model). The lack of spontaneous modes before and after the main NTM shows

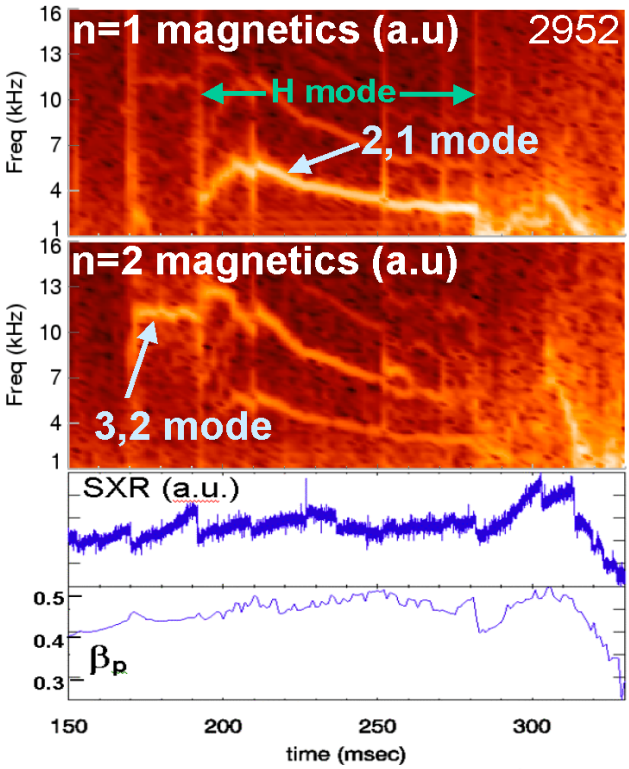

Fig 1: Typical NTM behaviour on MAST.

(denoted by poloidal/toroidal mode numbers). Mode numbers are clearly identified by magnetic arrays, with poloidal structure confirmed by 3D field modelling. Fig 2 shows how the modes clearly exhibit a critical β_p, typically ~0.4, with islands excited below this β_p usually decaying away. The 3/2 modes appear to have modest size (~4cm) and modest impact on confinement. However 2/1 NTMs are much larger in size (~10cm or ~15-20% of minor radius) and greater in effect, with large modes often associated with H-L mode back-transitions, and disruptions.

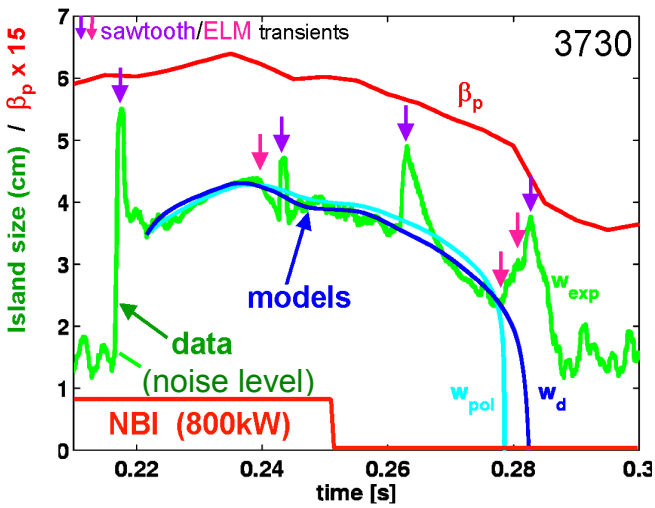

Fig 3: Evolution of a 3/2 NTM & model predictions

classical tearing stability ($\Delta'<0$). Modelling of this discharge went further, demonstrating that island evolutions could be reproduced with underlying physics parameters very close to values predicted by fundamental theory [3]. This is an important validation in a very different regime (low aspect ratio), significant not least because aspect ratio enters strongly into the various NTM underlying physics terms with a range of exponents. The modelling also highlights the role of field curvature effects as stabilising 60% of the bootstrap drive for the mode in this case. This beneficial effect for the ST was suggested from theoretical arguments in Ref [5], and with further development, it could provide a route to complete stabilisation of NTMs in the ST.

Further NTM research on MAST has considered the impact and avoidance of these modes. Early island size estimates were obtained from magnetic diagnostics, calibrated with 3D field modelling. This represented the island as a toroidally sinusoidal sheet current perturbation at the relevant rational surface, and used field line tracing to gauge island size. While this therefore correctly represented geometric effects it did not include the self-consistent response of the plasma to the mode. Nevertheless, effects of 3/2 modes, as in the case in Fig 2, appeared to show falls in stored energy consistent with the Chang and Callen type belt model approach, in which the island is assumed to flatten pressure gradients over its full width, leading to an energy reduction over the whole plasma core. New results from the 300 point Thomson scattering (TS) diagnostic have dramatically confirmed this picture for 2/1 modes that have magnetic amplitude, with large flat regions appearing in electron temperature and pressure profiles at the q=2 surface, as shown in Fig 4. The size of the flattening is very similar to magnetically based estimates. The flattening is not always observed, as it will depend on the exact phase of the island with respect to the TS line of sight - further studies will be interesting to explore the structure of the island.

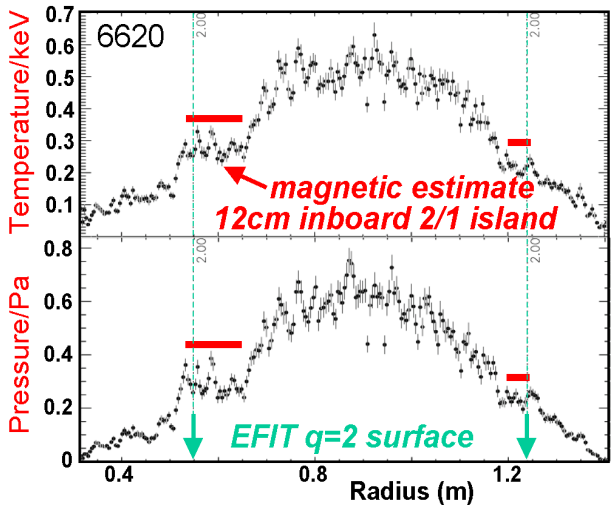

Fig 4: Island flattens Thomson scattering profiles

These n=1 tearing modes have a strong affect on the plasma. This can be most clearly discerned in cases where the mode occurs significantly later than the start of beam heating, an example of which is shown in Fig 5. Here the onset of the mode is associated with an abrupt cessation of stored energy rise (possibly this aspect may be associated with the onset of sawtoothing), and its continued growth leads to a ~25% fall in stored energy (which we attribute to the mode). The mode then locks and a disruption follows soon after. This appears to be the pattern of behaviour in most discharges: when large n=1 modes form they usually lock. Also, as shown in Fig 6 in the overwhelming majority of cases where n=1 modes lock, they usually progress to disruption. Note also that the locked modes seem to be localised towards low β_N values.

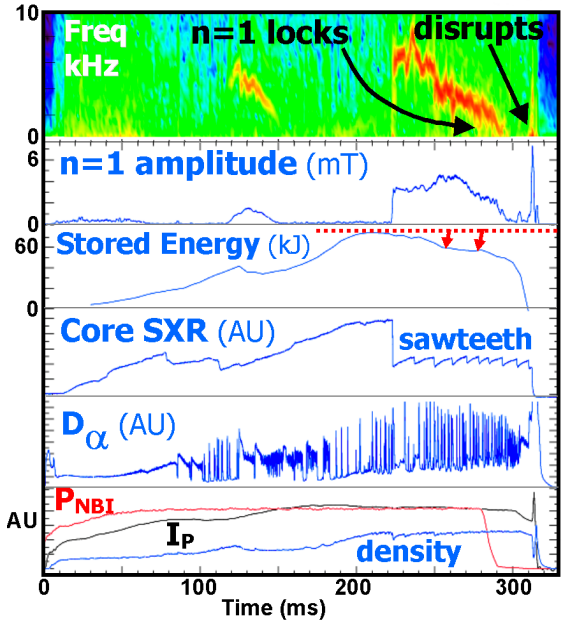

Fig 5: Effect of n=1 mode on plasma (#6228)

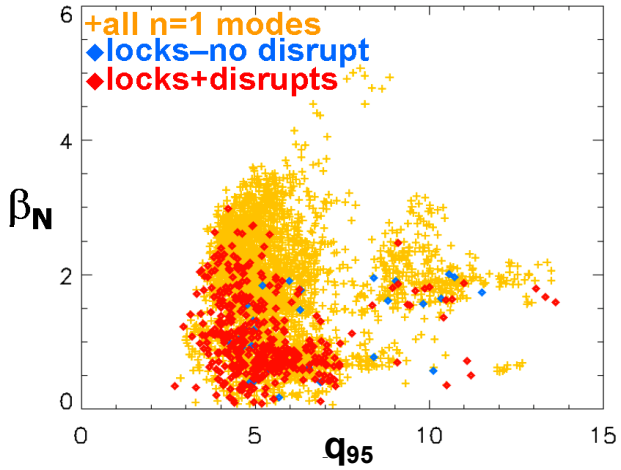

Fig 6: Incidence of locked modes and disruptions, plotted over all points where rotating n=1 modes exist (gold).

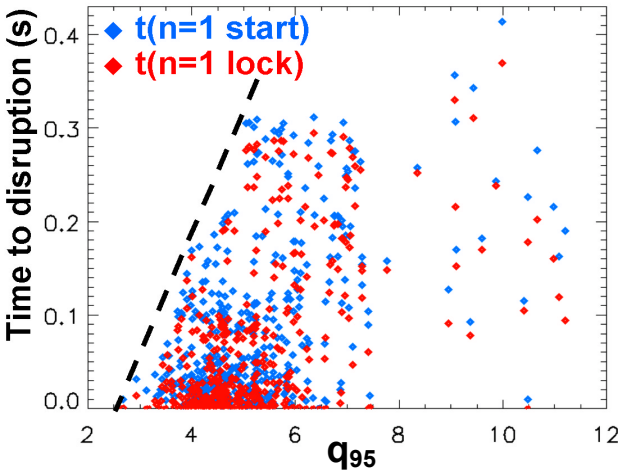

Fig 7: Time from mode start/lock to disruption

The disruptivity of the n=1 modes appears to scale with q_{95}, with modes at low q_{95} leading to disruptions more rapidly, as shown in Fig 7. This might be expected as the q=2 surface will be nearer the edge of the plasma at low q_{95} and so in a stronger pressure gradient region. It also indicates a possible role of error fields, with stronger coupling to the error field expected with larger q=2 radii. Further examination of the data set has also shown nearly all non-disruptive shots have q_{95} above 4 for their entire duration.

3. Error fields

The role of error fields has been explored in more detail in a series of low density Ohmic discharges. As shown in Fig 8, these exhibit classic (eg Ref [6]) error field induced mode behaviour. Unlike the cases above, no rotating modes are observed in the plasma prior to the appearance and growth of a locked mode (middle panel). The modes appear to grow linearly with time until a disruption is triggered. As expected for error field modes, there is a strong density dependence, with the later mode shots having higher density, and the disruption free case being the highest density of all, without a locked mode. There is no evidence for these modes being NTMs. Polar plots of saddle coil signals show a consistent ~4G response from the mode onset to just prior to the disruption, with the modes consistently orienting in one direction. An example of the locking is shown in Fig 9; here the amplitude of each of the 11 saddle loop signals is plotted in the radial direction with the value just prior to mode onset subtracted off, and radial position offset to constant

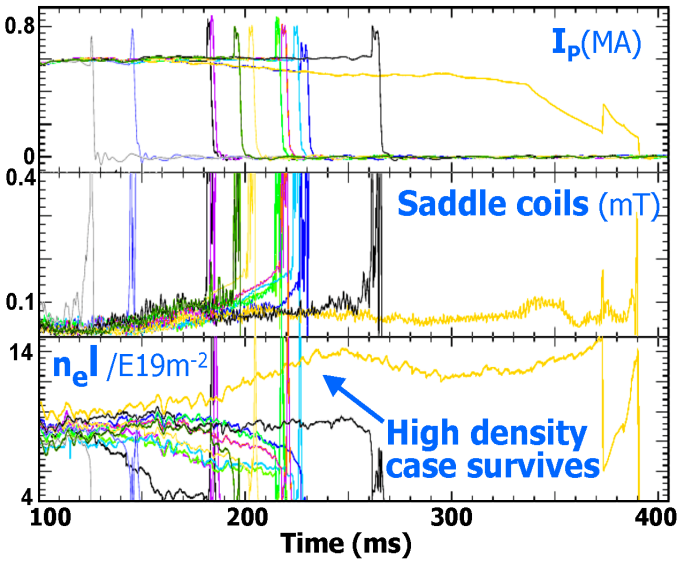

Fig 8: Time histories of low density Ohmic discharges.

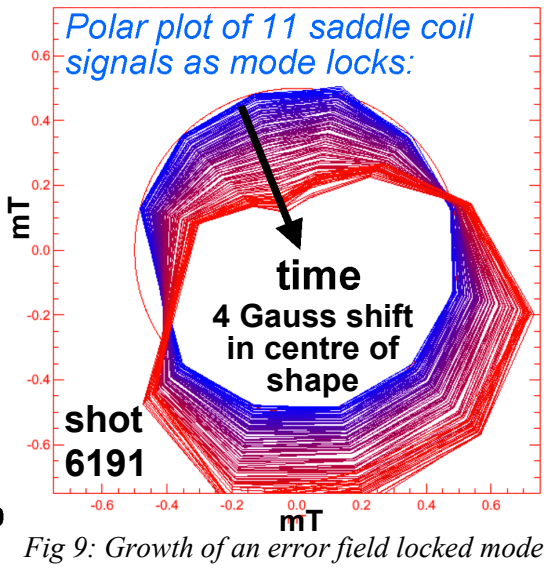

Fig 9: Growth of an error field locked mode observed on polar plot of saddle coil signals.

radius at the initial time. The angle of each point in the plot plane corresponds to the toroidal location of the detector. We find that as time progresses (indicated by colour) a systematic n=1 offset develops in the saddle loop signals. Low density limits due to error fields have been overcome somewhat by modifying the current ramp, and thus current profile evolution, and enabling faster rotation of the plasma. However, work has now commenced on the design of an error field correction system, to assist further current drive and other low density work on MAST.

4. NTM avoidance, high beta and ideal limits

The central role of the sawtooth in triggering NTMs on MAST, provides an effective tool for NTM avoidance - by controlling the sawtooth. By use of strong early neutral beam heating techniques, it should be possible to slow current diffusion times and so delay, or avoid completely, the onset of sawteeth, and therefore also prevent NTMs. (It is also possible that increased bootstrap and fast particle populations may play a role in current profile evolution and sawtooth stabilisation). This technique has been explored on MAST and has met with considerable success, producing some of the highest β_N and β_p plasmas to date. A good, but typical, example is shown in Fig 10. Here the sawteeth only appear once the beam heating is reduced, as evident from the SXR signals (earlier jumps have no inversion radius and are associated with ELMs). Note the MHD quiescent nature of this discharge - no large low m/n tearing modes are observed, and no disruption is triggered. Even in discharges from this series where sawteeth do appear earlier, their inversion radius is very small, and they do not trigger NTMs.

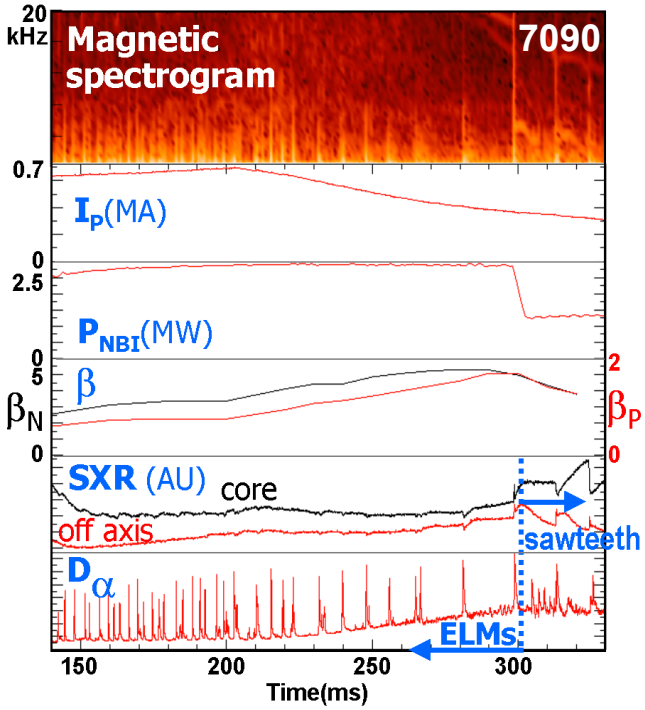

Fig10: High β is achieved by removal of sawteeth and tearing modes using strong early heating.

This has enabled very high β values to be produced with β_p reaching values of over 2 and β_N well in excess of 5. The most reliable estimates are obtained from kinetic measurements. In Fig 11 we show these for the highest β_p case, shot 7085 at 290ms. Electron pressure is taken from a 300 point Thomson scattering profile at this time. Charge exchange data shows ion temperatures average 50% higher than the electrons. The multi-chord visible bremsstrahlung is used to estimate a Z-effective value of 2.0±0.2, giving an electron to ion dilution factor of 0.78±0.05, assuming fully stripped Carbon. Folding this into a refined equilibrium calculation, using the CHEASE code [7], constrained to the EFIT magnetically reconstructed plasma boundary and total current

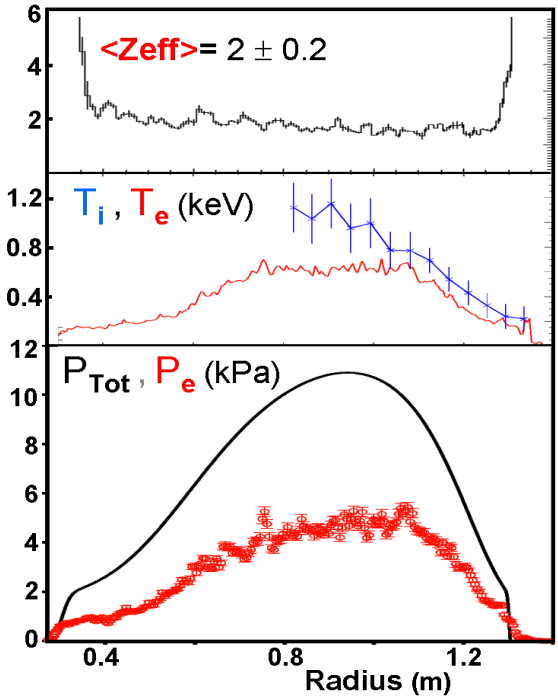

Fig 11: Profiles in #7085 at 290ms

profile, we obtain a thermal β_p of 2.1, β_N of 5.2, and a bootstrap fraction in the region 40-50%. This compares with EFIT magnetic reconstruction estimates of 1.95 and 4.7 at this time. Fast particle pressure has not been included in this calculation, as strong current ramp-down technique used to access this highest β_p renders the calculation less reliable for this particular case. However, in other discharges typical fast particle stored energies were ~20% of the total stored energy. The full parameter space is shown in Fig 12a. We see that MAST is now accessing plasmas with $\beta_N > 5$ and $\beta_N > 5l_i$, with validated EFIT reconstructions giving the highest β_N=5.3, highest β_p=1.95 and highest β_T =16% (note that EFIT estimates appear conservative compared to kinetics and fast particle modelling). The highest β_N are very close to the stability limit for the ideal no-wall pressure driven kink mode (within error bars for kinetic estimates). This was calculated with the KINX stability code [8], which computes linear ideal MHD growth rates for axisymmetric plasmas. However, we conclude that the absence of a large event in these discharges indicates that MAST has not quite reached this limit yet. Fig 12b shows that stability calculations are consistent with previous calculations, using PEST, by Menard [9], and indicates the route to higher stable performance is via broader pressure profiles.

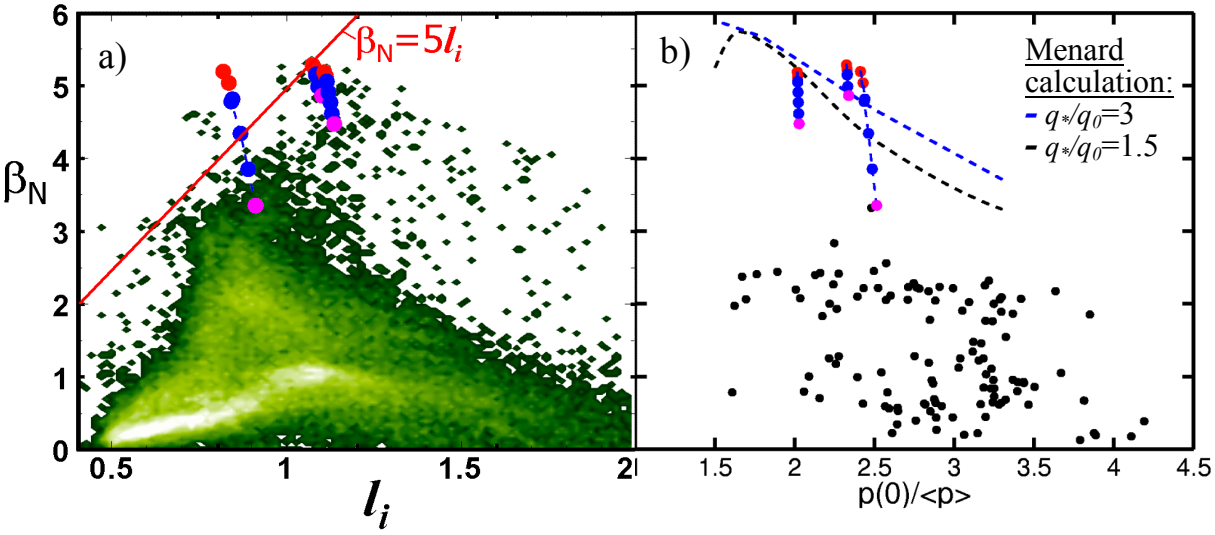

*Fig 12: Parameter space accessed to date on MAST (*EFIT *values): (a) β_N vs l_i over whole space; (b) β_N vs pressure peaking factor for random selection of shots. Overlaid are stability calculations: experimental thermal β value (pink); ideal MHD stable (blue); ideal MHD unstable (red). Dashed lines in (b) indicate Menard's limits for different q_*/q_0 (MAST values vary between these).*

5. Sawtooth physics

As we have seen, the role of the sawtooth is important in triggering NTMs. In the ST it might also be expected to have a significant effect in its own right, as the q=1 surface is often large in the ST, and indeed a broad flat central region is often observed on Thomson scattering profiles. Thus sawtooth effects were studied in carefully matched discharges, where only beam timing was changed to alter the sawtooth onset time. These are shown in Fig 13, where we observe that the stored energy is 10-15% higher in the non-sawtoothing case. This is confirmed by the Thomson scattering profiles shown in Fig 14. Further studies of the sawtooth show that it is not a Kadomtsev-type full reconnection in the ST. This is highlighted by a large number of cases where q=1 snakes co-exist with the sawtooth. The snakes have a clear m=1 structure, and become highly

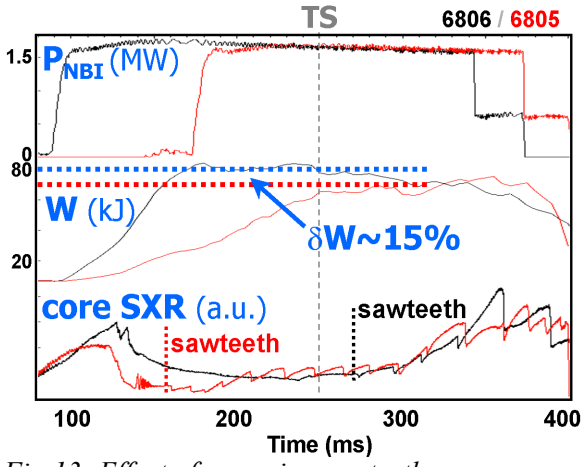

Fig 13: Effect of removing sawteeth on energy.

poloidally localised as they grow. An example of this is shown in Fig 15, where the snake starting at 111ms provides a clear marker for the q=1 surface. The sawteeth, commencing at 122ms, are observed to modulate the q=1 radius, but only by ~5-20%. Such data provides a good basis to test other physics models of the sawtooth. In particular, the Gimblett-Hastie model [10] proposes a secondary resistive interchange instability, triggered by some other event. This could have the effect of reducing pressure gradients in the core, without expelling the q=1 surface. Using carefully constrained reconstructions at the Thomson scattering time-point (141ms), just prior to a sawtooth crash, the modelling [7] indicates a region of resistive interchange instability extending just beyond the q=1 surface. This is comparable with the observed sawtooth inversion radius, and indicates the viability of this model, but is not yet compelling proof. Further studies are focusing on the triggering and post-crash states, while experimentally, higher elongation plasmas will allow better discrimination between the resistive interchange marginally unstable surface and q=1. Thus although there remains much to investigate, it shows how MAST can address this important issue.

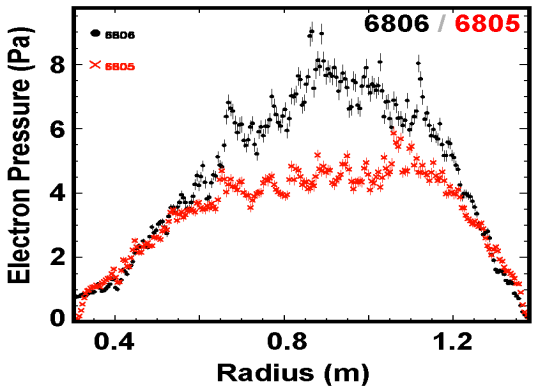

Fig 14: Effect of sawteeth on pressure profile

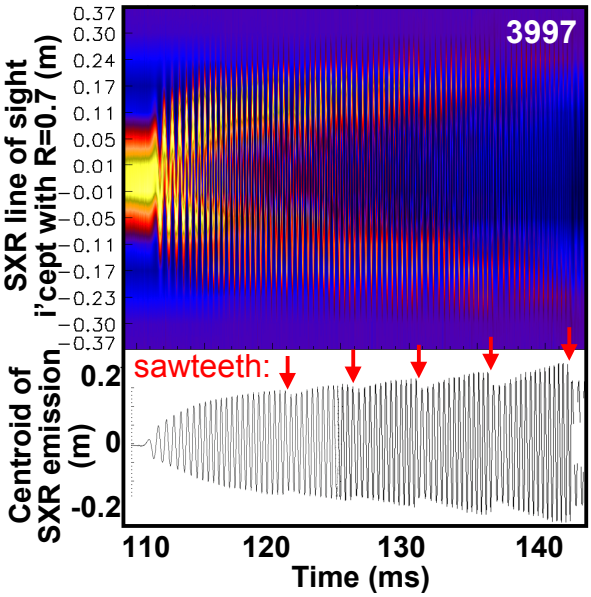

Fig 15: Effect of sawteeth on q=1 snake

6. Stability of Edge Localised Modes

A significant impact on the performance of H-mode plasmas comes from ELMs, with higher ELM frequencies associated with a clear fall-off in H factors. The ELM phenomenology is discussed in more detail in Ref [11], but they clearly exhibit many of the properties of type III ELMs, with energy losses in the 1-4% range, despite achieving values of $H_{IPB98Y2}$ up to and above 1. An initial examination of the ELMs shows them to be close to the n=∞ ballooning boundary (see Fig 16), suggesting proximity to regimes where type I ELMs might be expected. However, detailed modelling of a particular case, #6252 marked by the star, is illuminating. Here very accurate reconstructions of the plasma [7] have been obtained via careful matches to EFIT and a 300 point Thomson scattering profile which, most critically, provides good edge resolution. Ion pressure is assumed equal to electron pressure (a reasonable estimate based on Z-effective and charge exchange measurements). Current profiles from EFIT are modified near the edge by a second equilibrium code that calculates the bootstrap current (which is dominant near the edge) and

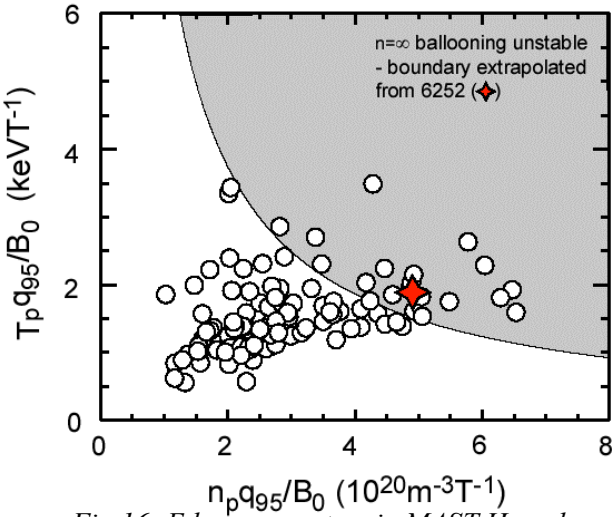

Fig 16: Edge parameters in MAST H modes compared with n=∞ ballooning boundary

re-converges to obtain a self-consistent representation of the plasma. This is then fed into the ELITE edge MHD stability code. ELITE identifies instability to peeling modes, with no coupling to sideband harmonics associated with ballooning modes; this is consistent with the concept of these being type III ELMs. As shown in Fig 17, the resulting eigenfunctions are very localised. Therefore, to explain the 2.6% stored energy loss observed with these ELMs there must be an avalanche process involved, if the peeling mode is the trigger. To explore whether large type I ELMs can be triggered on MAST, we artificially increased the pressure profile by ~50%. However the unstable modes remained localised, with little ballooning character, despite edge pressure gradients being well in excess of the $n=\infty$ ballooning limit. One interpretation is that the (stabilising) finite n corrections are important for narrow pedestal widths. This suggests that a broader pedestal would be more likely to be unstable to ballooning-type modes, and may provide a possible route for exploring large type I ELMs on MAST. An important message from this is that the type I-III ELM boundary does not just depend on simple $n=\infty$ ideal ballooning stability, and stabilising finite n corrections can be important for narrow pedestals. The results have important implications for other tokamaks, such as ITER, suggesting that narrow pedestals can accommodate steeper pressure gradients than might be expected from $n=\infty$ ballooning theory.

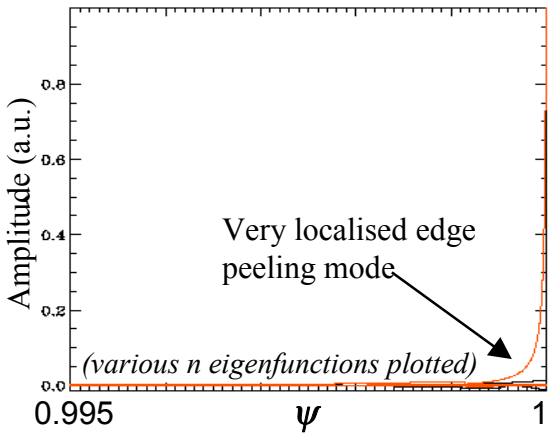

Fig 17: Eigenfunction of peeling mode for shot 6252, plotted vs normalised flux.

7. Conclusions

Large strides have been made on MAST in addressing issues of stability physics. The physics of the NTM has been explored, with behaviour used to test conventional physics models. The strong sawtooth seeding process on MAST and excitation of modes close to their marginal β_p, shows MAST to be a key facility for exploring the physics of NTM onset. By removing sawteeth, MAST has demonstrated how to avoid NTMs, and achieve high β_N and β_p. Calculations indicate that the MAST operation space now spans virtually the whole region below the no-wall ideal stability limit. Sawteeth have a modest effect on confinement. They do not appear to remove the q=1 surface in the ST, and behaviour is being used to test promising alternate models of behaviour. Finally ELM physics has been explored, with peeling/ballooning concepts tested against MAST data. This shows that narrow pedestals can accommodate steeper pressure gradients than might be expected from $n=\infty$ ballooning theory.

References

[1] LLOYD, B., et al., 'Overview of recent experimental results on MAST', this conference.
[2] SYKES, A., et al., Phys. Rev. Lett. **84** (2000) 495.
[3] BUTTERY, R. J., et al., Phys. Rev. Lett. **88** (2002) 125005.
[4] SAUTER, O., et al., Phys. Plasmas **4** (1997) 1654.
[5] KRUGER, S. E., HEGNA, C. C., and CALLEN, J. D., Phys. Plasmas **5** (1998) 455.
[6] BUTTERY, R. J., et al., Nucl. Fus. **40** (2000) 807.
[7] LUTJENS, H., et al., Comput. Phys. Commun. **97** (1996) 219.
[8] DEGTYAREV, L., et al., Comp. Phys. Com. **103** (1997) 10.
[9] MENARD, J., et al., Nucl. Fus. **37** (1997) 595.
[10] GIMBLETT, C. G., and HASTIE, R. J., Plas. Phys. Control. Fus. **36** (1994) 1439.
[11] COUNSELL, G. F., et al., 'Exhaust, ELM, and Halo Phys…', EX/D1-2, this conference.

This work was jointly funded by the U.K. Dept. of trade and Industry and EURATOM.